ANALYTICAL AND NUMERICAL CALCULATIONS OF PHOTOCONDUCTIVITY IN POROUS SILICON

L.S. MONASTYRSKII, B.S. SOKOLOVSKII, M.R. PAVLYK

Ivan Franko National University of Lviv
(50, Dragomanov Str., 79005 Lviv, Ukraine; e-mail: m.pavlyk@meta.ua*)*

PACS 73.50.Pz, 81.05.Rm, 07.05.Tp

The results of analytical and numerical calculations of photoconductivity in porous silicon with spherical and cylindrical pores are reported. The dependence of photoconductivity on the surface recombination rate has been analyzed for various pore radii, r_0, and various average distances between pores, $2R$. The photoconductivity of porous silicon increases with the distance between pores and decreases, as the pore radius or the surface recombination rate grows. In the case of small R/r_0 ratios, there is a significant discrepancy between the results of analytical calculations and those obtained numerically within the finite element method. The discrepancy was reduced to 1% by introducing a correction coefficient into the analytical expression.

1. Introduction

Today, porous materials are actively studied and used. In particular, it is porous silicon, which is classed, depending on the pore dimensions, to microporous (≤ 2 nm), mesoporous (2–50 nm), and macroporous (> 50 nm). Porous silicon is characterized by a large effective surface (200 m^2/cm^3). Therefore, the adsorption of chemically active molecules can result in a considerable variation of the charge carrier concentration, electric conductivity, photoconductivity, and luminescence. Large interest is attracted by a variation of the photoconductivity in porous silicon under the influence of external factors, e.g., various gas environments. Therefore, these structures can be used as effective gas sensors [1–4]. For designing and fabricating such sensors with required parameters, it is necessary to know the dependence of the photoconductivity of porous silicon on its surface properties, which change under the influence of a gas environment, the average pore diameter, and the distance between pores.

The problem of the photoconductivity in porous silicon has been considered in many works [5–7]. However, the detailed calculations, which would predict the dependence of the photoconductivity on the pore dimensions and the geometry under conditions of the rather intensive recombination of photocarriers on the pore surface, are absent. In works [8, 9], an analytical model of photoconductivity in macroporous silicon was proposed, but its scope of validity was not marked accurately. Therefore, in this work, we carried out a computer simulation of the photoconductivity in macroporous silicon with spherical and cylindrical pores. We found that the analytical approach can be used while solving this problem, provided that the relevant correction coefficients are introduced.

2. Photoconductivity of Macroporous Silicon with Spherical Pores

Consider a model of semiconductor with p-type conductivity, in which spherical pores are regularly arranged. The pore radius is r_0, and the average distance between pore centers is $2R$. We assume that the semiconductor is illuminated with light that generates electron-hole pairs, the concentration of which, G, does not depend on the coordinate. As a result of the strong photocarrier recombination on the pore surface, there emerges a non-uniform distribution of photocarriers in the semiconductor, so that photocarriers diffuse ambipolarly toward pores. In the case of spherical symmetry, the spatial distribution of the photocarrier concentration Δn in the interval $r_0 \leq r \leq R$ is described by the equation

$$\frac{d^2\Delta n}{dr^2} + \frac{2}{r}\frac{d\Delta n}{dr} - \frac{\Delta n}{L_n^2} = -\frac{\tau_n G}{L_n^2}, \qquad (1)$$

where L_n is the electron diffusion length, and τ_n is the electron lifetime. Note that, for macroporous silicon, $L_n \sim 10^{-7}$ m and $\tau_n \sim 10^{-6}$ s [10]. Equation (1) should be supplemented with two boundary conditions. The first condition describes the recombination of carriers on the pore surface,

$$\frac{d\Delta n(r_0)}{dr} = \frac{S\tau_n}{L_n^2}\Delta n(r_0), \tag{2}$$

where S is the surface recombination rate of photocarriers, which depends on the physical and chemical states of the pore. For instance, it may depend on the presence of gas molecules in the pores, which can change the electrostatic potential and, as a consequence, the rate of photocarrier recombination. The second boundary condition follows from the fact that the photocarrier concentration attains its maximal value at the middle point between the pores,

$$\frac{d\Delta n(R)}{dr} = 0. \tag{3}$$

The analytical solution of Eq. (1) with boundary conditions (2) and (3) is

$$\frac{\Delta n(r^*)}{G\tau_n} = 1 - \left\{ S^* r_0^* \left[\left(1 + \frac{1}{R^*}\right) \exp(r^* - R^*) + \right.\right.$$

$$\left. + \left(1 - \frac{1}{R^*}\right) \exp(-r^* - R^*) \right] \Bigg/$$

$$\Bigg/ 2r^* \left\{ \left[\frac{1}{r_0^*} - \frac{1}{R^*} + S^* \right] \cosh(R^* - r_0^*) - \right.$$

$$\left.\left. - \left[\frac{1}{r_0^* R^*} - 1 + \frac{S^*}{R^*} \right] \sinh(R^* - r_0^*) \right\} \right\}, \tag{4}$$

where

$$R^* = \frac{R}{L_n},\ r_0^* = \frac{r_0}{L_n},\ r^* = \frac{r}{L_n},\ S^* = \frac{S\tau_n}{L_n}$$

are dimensionless quantities.

The formula for the average photocarrier concentration $\langle \Delta n \rangle$, which corresponds to the photoconductivity of porous silicon, is as follows [8]:

$$\frac{\langle \Delta n \rangle}{G\tau_n} =$$

$$= 1 - \frac{R^{*3}(6-\pi)(1-\Delta n(R^*)) + 3\pi r_0^{*2} S^* \Delta n(r_0^*)}{6R^{*3} - \pi r_0^3}. \tag{5}$$

Using the finite element method [11], we obtained numerical solutions of Eq. (1) with the boundary conditions (2) and (3) in the general case where no spherical symmetry was assumed. These solutions are represented as the dependences of the photoconductivity in porous silicon on the pore radius and the ratio between the pore-to-pore distance and the pore radius for various rates of surface recombination (Figs. 1,*a* and *b*).

The photoconductivity of porous silicon grows, if the distance between pores increases, and decreases, if either the pore radius or the rate of surface recombination grows. The results of calculations show that the values obtained numerically are larger. The difference between the numerical and analytical results of calculations diminishes, as the distance between pores increases.

At small distances between pores, the analytical method gives a considerable error of 50–60% with respect to the numerical results (see Fig. 2, curves 1 and 2). To reduce the error, we can make the substitution $R^{**} = R^*/a$, where $a = 0.73$ [8], in the expression for the photoconductivity,

$$\frac{\langle \Delta n \rangle}{G\tau_n} =$$

$$= 1 - \frac{R^{*3}(6-\pi)(1-\Delta n(R^{**})) + 3\pi r_0^{*2} S^* \Delta n(r_0^*)}{6R^{*3} - \pi r_0^3}. \tag{6}$$

In the calculation of the average photocarrier concentration $\langle \Delta n \rangle$, an "elementary cell" in the semiconductor was selected, which is represented by a cube with the side length $2R^*$. The number of photocarriers in this cell was calculated. To consider the photocarriers in the regions belonging to the cube, but beyond the pore, it is possible, as the first approximation, to take the carrier concentration in these regions constant and equal to $\Delta n(R^{**})$, i.e. the concentration of photocarriers at the middle point between the pore and the cube vertex. As a result, the error diminished to 3–8% (Fig. 2, curves 3 and 4). Our calculations show that $\Delta n(R^*)$ calculated numerically exceeds the corresponding value obtained analytically. This circumstance is related to the fact that photocarriers drift out from the regions of the "elementary cell" located beyond the pore. A subsequent reduction of the error (to 1%) can be reached by introducing the corrected variables $R'^* = R^*/b$ and $R'^{**} = R^{**}/b$ into expression (6),

$$\frac{\langle \Delta n \rangle}{G\tau_n} =$$

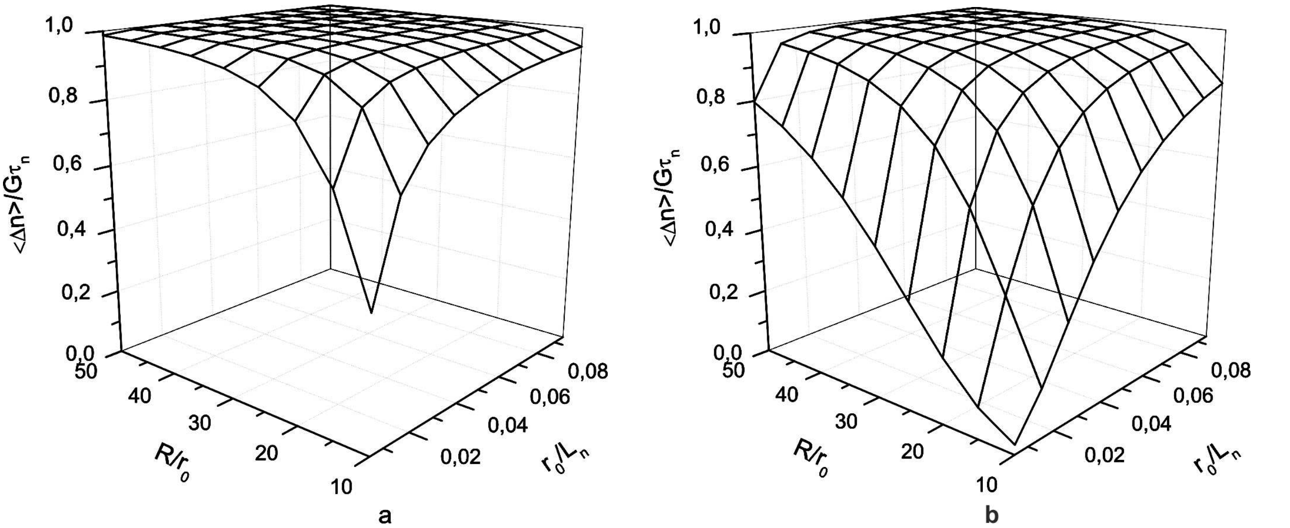

Fig. 1. Dependences of the photoconductivity on R/r_0 and r_0/L_n for various rates of surface recombination $S^* = 5$ (a) and 200 (b) for porous silicon with spherical pore geometry

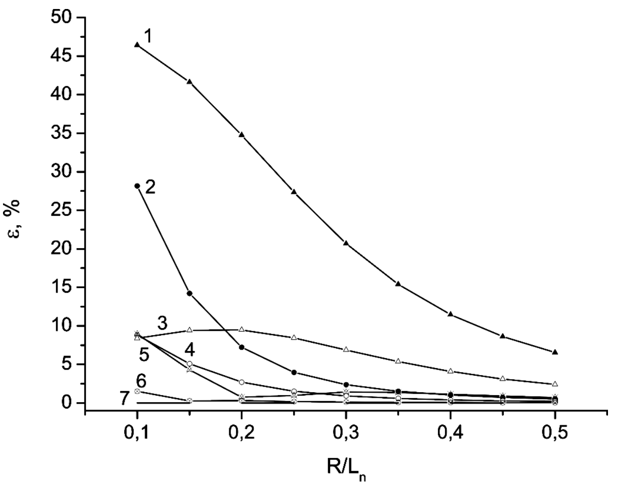

Fig. 2. Dependences of the relative difference $\epsilon = \left[\left(\frac{\langle\Delta n\rangle}{G\tau_n}\right)_{\rm num} - \left(\frac{\langle\Delta n\rangle}{G\tau_n}\right)_{\rm anal}\right]\left(\frac{\langle\Delta n\rangle}{G\tau_n}\right)^{-1}_{\rm num}$ between the numerical and analytical results on the photoconductivity on the distance between pores for various S^* at $r_0^* = 0.01$. Curves *1* and *2* are the errors of expression (5) at $S^* = 5$ and 200, respectively; curves *3* and *4* are the errors of expression (6) at $S^* = 5$ and 200, respectively; curves *5* and *6* are the errors for expression (7) with the averaged $b = 0.92$ at $S^* = 5$ and 200, respectively; curve *7* is the error of expression (7) with the coefficient b for various values of R/L_n and S^*

$$= 1 - \frac{R'^{*3}(6-\pi)(1-\Delta n(R'^{**})) + 3\pi r_0^{*2} S^* \Delta n(r_0^*)}{6R'^{*3} - \pi r_0^3}. \quad (7)$$

The coefficient b has to be selected so that the error should be less than 1% (Fig. 2, curve *7*) for various distances between pores R^*'s and rates of surface recombination S^*'s. Knowing the range of the coefficient b, we selected its averaged value 0.92. The error given by expression (7) with this b-value did not exceed 1–2% (Fig. 2, curves *5* and *6*).

3. Photoconductivity of Macroporous Silicon with Cylindrical Pores

Now consider a model of porous semiconductor of a unit thickness with parallel cylindrical pores of radius r_0 regularly arranged over the semiconductor bulk. The average distance between pore axes is $2R$. Let the problem have a cylindrical symmetry. Then, the spatial distribution of the photocarrier concentration Δn is described by the differential equation

$$\frac{1}{r}\frac{d}{dr}\left(r\frac{d\Delta n}{dr}\right) - \frac{\Delta n}{L_n^2} = -\frac{\tau_n G}{L_n^2}. \quad (8)$$

This equation is supplemented with boundary conditions (2) and (3). The analytical solution obtained by us for Eq. (8) with boundary conditions (2) and (3) is [9]

$$\frac{\Delta n(r^*)}{G\tau_n} = 1 -$$

$$- \frac{S^*[I_1(R^*)K_0(r^*) + K_1(R^*)I_0(r^*)]}{I_1(R^*)[K_1(r_0^*) + S^*K_0(r_0^*)] - K_1(R^*)[I_1(r_0^*) - S^*I_0(r_0^*)]}, \quad (9)$$

where I_n and K_n are the n-order Bessel functions with imaginary argument [12]. The expression for the deter-

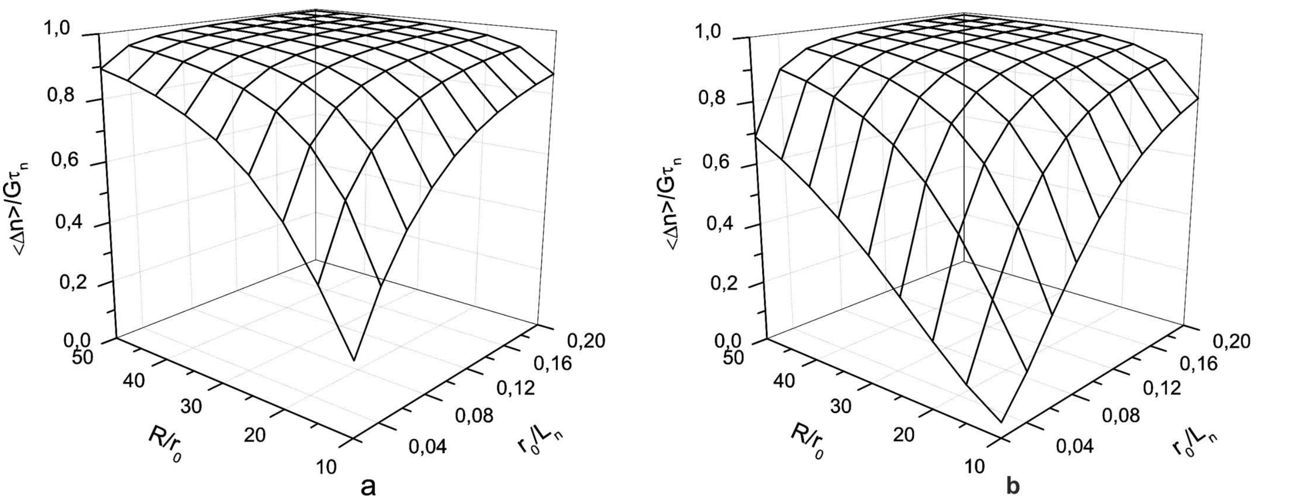

Fig. 3. Dependences of the photoconductivity on R/r_0 and r_0/L_n for various rates of surface recombination $S^* = 5$ (a) and 200 (b) for porous silicon with the cylindrical geometry of pores

mination of the average concentration $\langle \Delta n \rangle$ corresponding to the photoconductivity of porous silicon is

$$\frac{\langle \Delta n \rangle}{G\tau_n} = 1 - \frac{1}{4R^{*2} - \pi r_0^{*2}} \times$$

$$\times \left\{ \frac{2\pi r_0^* S^* \Delta n(r_0^*)}{G\tau_n} + R^{*2}(4-\pi) \left[1 - \frac{\Delta n(R^*)}{G\tau_n} \right] \right\}. \quad (10)$$

We used the method of finite elements to obtain solutions of Eq. (8) with boundary conditions (2) and (3) in the general case where no cylindrical symmetry was assumed (Figs. 3,a and b). The photoconductivity of porous silicon also grows in this model, if the distance between pores increases, and decreases, if the pore radius or the rate of surface recombination grows. Numerical results are higher. As the distance between pores increases, the difference between the numerical and analytical calculation results decreases.

The analytical calculations gives a substantial error of 20–30% with respect to the numerical results at small values of pore radius (Fig. 4, curves 1 and 2). To reduce the error, we can make the substitution $R^{**} = R^*/a$, where $a = 0.83$ [9], into the expression for the photoconductivity:

$$\frac{\langle \Delta n \rangle}{G\tau_n} = 1 - \frac{1}{4R^{*2} - \pi r_0^{*2}} \times$$

$$\times \left\{ \frac{2\pi r_0^* S^* \Delta n(r_0^*)}{G\tau_n} + R^{*2}(4-\pi) \left[1 - \frac{\Delta n(R^{**})}{G\tau_n} \right] \right\}. \quad (11)$$

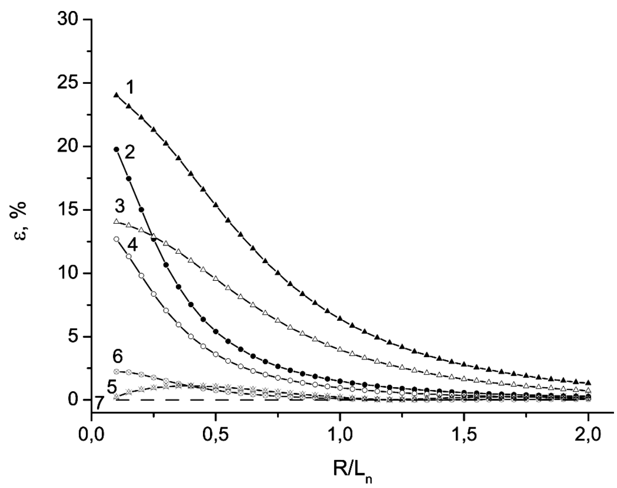

Fig. 4. Dependences of the relative difference ϵ between the numerical and analytical results on the photoconductivity on the distance between pores for various S^* at $r_0^* = 0.01$. Curves *1* and *2* are the errors of expression (10) at $S^* = 5$ and 200, respectively; curves *3* and *4* are the errors of expression (11) at $S^* = 5$ and 200, respectively; curves *5* and *6* are the errors for expression (12) with the averaged $b = 0.94$ at $S^* = 5$ and 200, respectively; curve *7* is the error of expression (12) with the coefficient b for various values of R/L_n and S^*

This substitution and the following one were fulfilled basing on the same reasons as were presented above. The difference is that an "elementary cell" was used in the form of a parallelepiped of unit height and with a square basis with the side length $2R^*$. As a result of this substitution, the error decreased to 5–15% (Fig. 4, curves 3 and 4). A subsequent reduction of the error (to 1%) can be reached by introducing the corrected variables

$R'^{*} = R^{*}/b$ and $R'^{**} = R^{**}/b$ into expression (12),

$$\frac{\langle \Delta n \rangle}{G\tau_n} = 1 - \frac{1}{4R'^{*2} - \pi r_0^{*2}} \times$$

$$\times \left\{ \frac{2\pi r_0^{*} S^{*} \Delta n(r_0^{*})}{G\tau_n} + R'^{*2}(4-\pi) \left[1 - \frac{\Delta n(R'^{**})}{G\tau_n} \right] \right\}. \quad (12)$$

The coefficient b is so selected to provide the error less than 1% (Fig. 4, curve *7*) for various values of the distance between pores R^{*} and the rate of surface recombination S^{*}. Similarly to what was done in the case of spherical geometry, we can take the averaged value $b = 0.94$. The corresponding error given by expression (12) was not larger than 1–5% (Fig. 4, curves *5* and *6*).

Note that the model proposed in this paper allows the experimental results of work [7] to be explained qualitatively. In particular, a growth of the photoconductivity maximum was observed at a porosity reduction, the latter being governed by the current density at the anode etching.

4. Conclusions

The photoconductivity of macroporous silicon at a fixed nonzero value of surface recombination rate is shown to grow with the average distance between pores and to diminish as the pore radius increases. The increase of the surface recombination rate at given values of pore radius and average distance between pores leads to a monotonous reduction of the photoconductivity which saturates at high rates of surface recombination.

Numerical calculations of the photoconductivity in macroporous silicon are carried out. By comparing those results with the results of analytical calculations, the averaged correction coefficients $b = 0.92$ and 0.94 were determined for the spherical and cylindrical, respectively, symmetries of the problem. The averaged coefficients b are used to obtain new analytical expressions for the photoconductivity in macroporous silicon, which gave an error of 1–5%. The analytical expressions without correction are found to give a large error at small distances between pores. At $R > L_n$, the error tends to 1%. This means that, if $R > 2.5L_n$, there is no necessity to carry out a correction in those expressions.

1. D.I. Bilenko, O.Yu. Belobrovaya, E.A. Zharikova, D.B. Terin, and E.I. Khasina, Fiz. Tekh. Poluprovodn. **39**, 834 (2005).
2. A. Bratkowski, F. Korcala, Z. Lukasik, P. Borowski, and W. Bal, Opto-Electron. Rev. **13**, 35 (2005).
3. C. Baratto, G. Faglia, G. Sberveglieri *et al.*, Sensors **2**, 121 (2002).
4. S.-J. Kim, J.-Y. Park, S.-H. Lee, and S.-H. Yi, J. Phys. D **33**, 1781 (2000).
5. L. Kaifeng, W. Yumin, Z. Lei *et al.*, Chin. Phys. Lett. **11**, 289 (1994).
6. V.I. Ivanov, L.A. Karachevtseva, N.I. Karas *et al.*, Semicond. Phys. Quant. Electron. Optoelectron. **10**, 72 (2007).
7. H. Khalili, R.S. Dariani, A. Morteza *et al.*, J. Mater. Sci. **42**, 908 (2007).
8. L.S. Monastyrskii, and B.S. Sokolovskii, Prikl. Fiz. **6**, 127 (2007).
9. L.S. Monastyrskii, B.S. Sokolovskii, and V.S. Vasylyshyn, Opt. Mem. Networks **18**, 55 (2009).
10. A.J. Simons, in *Properties of Porous Silicon*, edited by L. Canham (INSPEC, London, 1997), p. 176.
11. O.C. Zienkiewicz, R.L. Taylor, and J.Z. Zhu, *The Finite Element Method: Its Basis and Fundamentals* (Elsevier Butterworth-Heinemann, Oxford, 2005).
12. G.N. Watson, *Theory of Bessel Functions* (Cambridge Univ. Press, Cambridge, 1962).

Received 13.01.11.
Translated from Ukrainian by O.I. Voitenko

АНАЛІТИЧНІ ТА ЧИСЕЛЬНІ РОЗРАХУНКИ ФОТОПРОВІДНОСТІ ПОРУВАТОГО КРЕМНІЮ

Л.С. Монастирський, Б.С. Соколовський, М.Р. Павлик

Р е з ю м е

Представлено результати аналітичного та чисельного розрахунків фотопровідності макропоруватого кремнію зі сферичними і циліндричними порами. Проаналізовано залежність фотопровідності від швидкості поверхневої рекомбінації при різних радіусах пор (r_0) та середніх відстанях ($2R$) між ними. Фотопровідність поруватого кремнію зростає при збільшенні відстані між порами і зменшується при зростанні радіуса пор або швидкості поверхневої рекомбінації. Показано, що у випадку малих значень відношень R до r_0 між результатами аналітичного розрахунку та чисельного моделювання методом скінченних елементів існує суттєва різниця, яку зменшено (до 1%) шляхом введення коректуючого коефіцієнта в аналітичний вираз.